

Radiation



Technical Note

Radiation Characteristics of Traffic Radar Systems



RADIATION CHARACTERISTICS OF TRAFFIC RADAR SYSTEMS

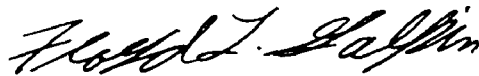
Norbert N. Hankin

March 1976

U.S. Environmental Protection Agency
9100 Brookville Road
Silver Spring, Maryland 20910

PREFACE

The Office of Radiation Programs of the Environmental Protection Agency carries out a national program designed to evaluate population exposure to ionizing and nonionizing radiation, and to promote the controls necessary to protect the public health and safety. This report gives the results of measurements and calculations of the microwave power density produced by typical traffic radar systems. Readers of this report are encouraged to inform the Office of Radiation Programs of any omissions or errors.



Floyd L. Galpin, Director
Environmental Analysis
Division (AW-461)

RADIATION CHARACTERISTICS OF TRAFFIC RADAR SYSTEMS

Norbert N. Hankin
U.S. Environmental Protection Agency
9100 Brookville Road
Silver Spring, Maryland 20910

INTRODUCTION

This study reports the results of measurements and calculations of microwave radiation power density produced by typical traffic radar systems.

CHARACTERISTICS OF SYSTEMS STUDIED

Traffic radar systems are small portable units used by police (in both moving or stationary modes) to determine the speed of vehicles relative to that of the police vehicles in which the units are mounted. True ground speed is obtained by correcting for the speed of the police vehicle. The system operation is based upon measuring the Doppler shift in the fundamental CW frequency transmitted; the shift in frequency being directly related to the relative velocity of the target vehicle and the microwave radiation source.

The specific systems studied appear to represent the majority of traffic radars in use. The microwave source, radiation frequency, source power, and antenna are typical for this type of microwave system and appear relatively independent of manufacturer. Four different commercially available traffic radar microwave systems were studied, the only difference between systems being the antenna dimensions. Commercially available systems appear to differ primarily in electronic circuitry, data acquisition and reduction, and system packaging, but very little in microwave source characteristics.

Measurements to obtain radiation characteristics data were performed on the MR7 Moving Radar (Kustom Signals, Inc., Chanute, Kansas). Determination of radiation characteristics by analysis, done for the MR7, was found to be in good agreement with measurement results. This analysis was then used to study the MOVAR Moving Radar System (CMI, Inc., Chanute, Kansas).

The characteristics of the microwave systems studied are presented in Table 1.

ANALYSIS OF ANTENNA RADIATION CHARACTERISTICS

The antenna used to transmit microwave radiation with the spatial distribution (radiation pattern) desired for traffic radars is the conical horn antenna. Experimentally determined radiation characteristics of this type of antenna are available [1] to be used in an analysis of specific system characteristics.

The significant characteristic to be determined in evaluating a traffic radar system, relative to its capability to create biologically significant environmental radiation levels, is the maximum power density of the microwave radiation which can be produced, at any distance from the antenna, and to which individuals may be exposed. The mathematical relationships and generalized characteristics which describe the radiation properties of

Table 1. System Characteristics

Characteristic	MR7, TR6*	MOVAR, Speedgun II**
Antenna type	Conical horn	Conical horn
Antenna dimensions		
diameter (inches)	6.5	4
length (inches)	18	9
Radiation polarization	Circular	Circular
Radiation source	Gunn diode	Gunn diode
RF power (W)	0.02 (min)	0.02 (min)
	0.1 (max)	0.1 (max)
RF frequency (GHz)	10.525 \pm .025	10.525 \pm .025
Half power beam width (deg)	12	14 to 16

*MR7 Moving Radar System and TR6 Traffic Radar System are produced by Kustom Signals, Inc., Chanute, Kansas.

**MOVAR Moving Radar System and Speedgun II are produced by CMI, Inc., Chanute, Kansas.

conical horns [1] are used to determine the far field power density produced by the systems included in Table 1.

The maximum value of power density exists on the antenna axis. The far-field power density, W_{ff} , due to a radiation source is given by Equation 1 in terms of antenna gain relative to an isotropic radiator, the transmitter power available for radiation, and the distance between the source and field point.

$$(1) \quad W_{ff} = \frac{P \cdot G}{4\pi R^2}$$

W_{ff} = far field power density, Watt/m²

P = radiated power, Watt

R = source-field point separation distance, m

G = antenna gain relative to an isotropic radiator

This is based upon the concept that in the far-field the source appears to be a point source. The gain of a conical horn depends upon the horn diameter, D, the radiation wavelength, λ , and the relationship between the flare length, l , and the aperture diameter which determines the phase deviation, s , in the aperture wavefront. The gain, G, may be calculated by the following relationship (Equation 2).

$$(2) \quad G \text{ (dB)} = 20 \log\left(\frac{\pi D}{\lambda}\right) - L$$

The gain-correction factor L is dependent upon these parameters as shown in Figure 1.

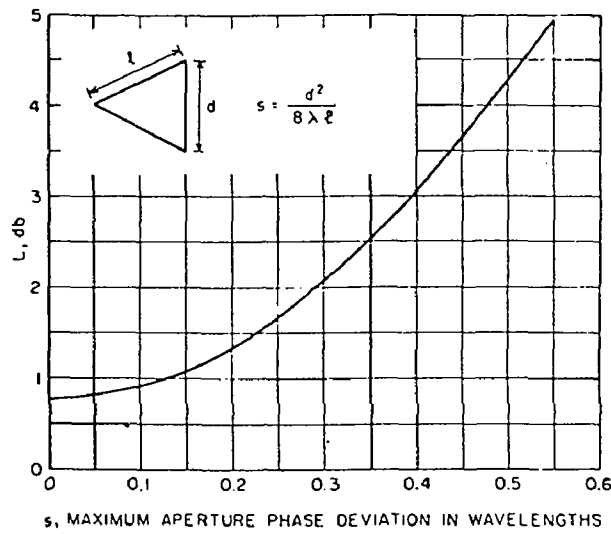


Fig. 1. Gain-correction factor for conical horn [1]

Off-axis power density levels are determined by using experimentally determined radiation patterns which consist of graphs of relative field strength (normalized to the maximum on-axis value) as a function of angle relative to the antenna axis. The power density of the electromagnetic radiation field is proportional to the square of the field strength; therefore off-axis power density at a given distance from the source is obtained by use of Equation 3.

$$(3) \quad W_{ff}(\theta) = W_{ff}(R_\theta)^2$$

where $W_{ff}(\theta)$ is the off-axis far field power density at an angle θ , W_{ff} is the on-axis far field power density at the same distance from the antenna, and R_θ is the relative field strength at an angle θ relative to the antenna axis.

Empirically determined radiation patterns for various conical horns are presented in Figure 2 [1].

These curves may be used in calculating off-axis power density for conical horns having dimensions different from the horns shown, but whose dimensions (diameter and flare length) produced the same phase deviation as one of the given horns; however, the abscissa scale angle must be changed. For a horn with dimensions different than any of those shown, the phase deviation (in number of wavelengths) is determined by Equation 4.

$$(4) \quad s = \frac{D^2}{8\lambda l}$$

This phase deviation is compared to those for the specific horns of Figure 2, and the radiation pattern of the one whose phase deviation most nearly approximates s is selected to be used in determining the relative field intensity vs. θ for the conical horn of interest. The angular position θ in the far field is related to θ_1 of the horn selected in Figure 2 by Equation 5.

$$(5) \quad \sin \theta = \frac{\lambda D_1}{\lambda_1 D} \sin \theta_1$$

where λ , D , and θ are quantities referring to the horn of interest and λ_1 , D_1 , and θ_1 refer to the horn whose radiation patterns are given in Figure 2.

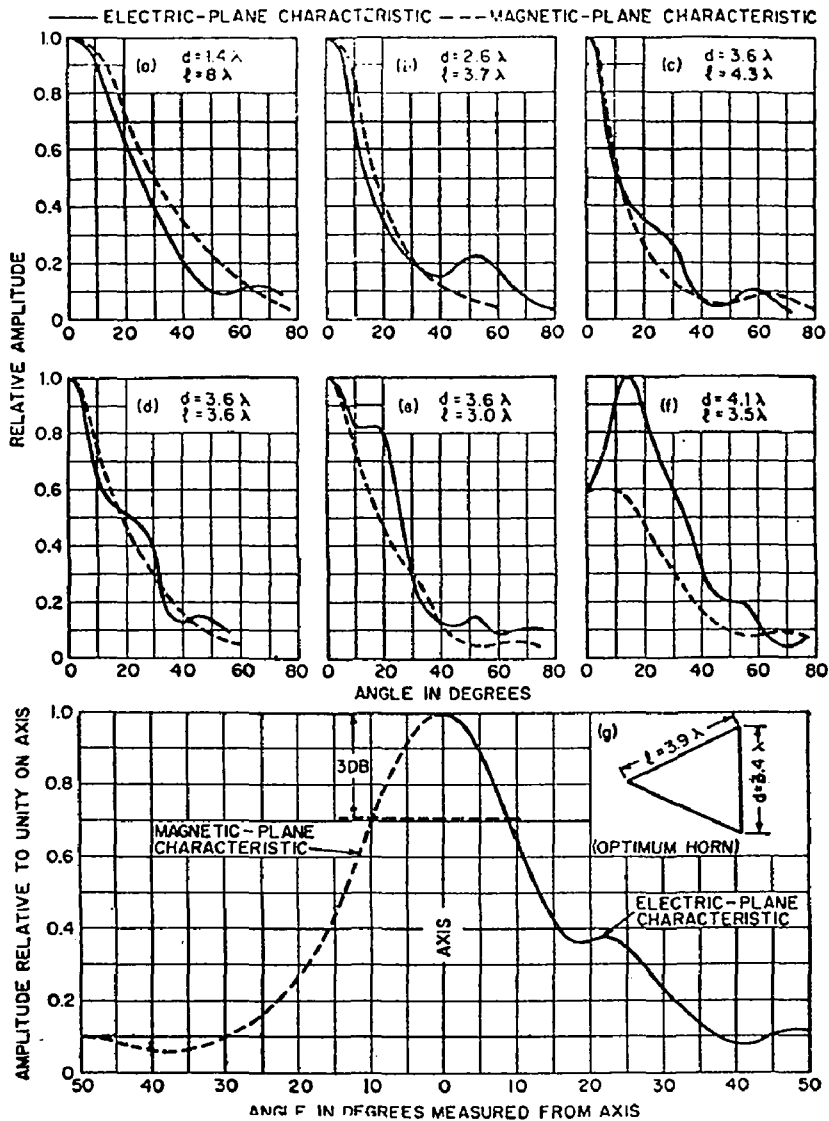


Fig. 2 Observed radiation patterns for conical horns of various dimensions

ANALYTICALLY DETERMINED FAR FIELD RADIATION LEVELS: POINT SOURCE MODEL

The far-field, on-axis power density produced by the traffic radar systems, listed in Table 1, can be determined using the expressions for far field power density, Equation 1, conical horn gain, Equation 2, and gain-correction factors, Figure 1. The half-power beam width, first sidelobe power density relative to main beam maximum power density, and angular position of the first sidelobe relative to antenna axis can be approximately calculated using the appropriate curve in Figure 2. Power density determination is based upon assuming a total radiated power of 0.1 Watt, the maximum power of the microwave source. Table 2 summarizes the pertinent system characteristics thus determined using the radiation pattern of horn (b), Figure 2, for beamwidth and sidelobe characteristics.

The calculated on-axis power densities which would be expected at various distances from the antenna, and the main beam diameter across the half-power points (beamwidth, cm) are presented in Table 3.

ANALYTICALLY DETERMINED CHARACTERISTICS: CIRCULAR APERTURE MODEL

The expression for the gain (Equation 2) of a conical horn can be shown to be the theoretical gain, G_0 , of a uniformly illuminated circular aperture, the maximum

Table 2. System Characteristics Required for Far-Field Calculations

System	Horn Diameter (cm)	Flare Length (cm)	Phase Deviation $= \frac{D^2}{8\lambda l}$	G_0 (dB)	L (dB)	G (dB)	Beam Width (deg)	First sidelobe Angle (deg)	First sidelobe Rel. levels (dB)
TR6, MR7	16.5	45.7	.261	25.2	1.75	23.4	8.9	20.7	-14
MOVAR, Speedgun	10.2	22.9	.198	21.0	1.34	19.7	14	34.9	-14

Table 3. Calculated Power Density and Beam Width

System	Characteristic	Distance (m)				
		.66	.91	1.32	2.67	28.3
TR6, MR7	W_{ff} (W/m ²)	4	2.1	1	2.44×10^{-1}	2.17×10^{-3}
	Beam Width (cm)	13.9	19.1	27.7	56.1	595
MOVAR, Speedgun	W_{ff} (W/m ²)	1.70	8.97×10^{-1}	4.26×10^{-1}	1.04×10^{-1}	9.27×10^{-4}
	Beam Width (cm)	16.2	22.3	32.4	65.6	695

possible gain which occurs for constant phase distribution over the aperture, corrected for phase deviation over the aperture. The over-all gain of an aperture may be expressed as Equation 6

$$(6) \quad G = \eta G_0$$

where η is the efficiency (gain factor) of the aperture, a measure of the effectiveness of the antenna in collimating available radiation energy into the peak of the main lobe in the far field of the aperture [2,3]. The theoretical gain, G_0 , is expressed as

$$(7) \quad G_0 = \frac{4\pi A}{\lambda^2}$$

when A is the aperture area. The reduction in actual gain compared to theoretical gain may be considered to be a reduction in the illuminated aperture area; i.e.,

$$(8) \quad A_{eff} = \eta A = \frac{G\lambda^2}{4\pi}$$

where A_{eff} is the effective aperture area being uniformly illuminated.

Relating the expression for the gain of a conical horn to that for a non-uniformly illuminated circular reflector may be accomplished by using Equations 6 and 7 to express actual gain as

$$(9) \quad G = \eta \frac{4\pi A}{\lambda^2} = \eta \cdot \frac{4\pi}{\lambda^2} \cdot \frac{\pi D^2}{4} = \eta \left(\frac{\pi D}{\lambda} \right)^2$$

The gain expressed in decibels, dB, is

$$(10) \quad G_{dB} = 10 \log_{10} G = 10 \left(2 \log_{10} \left(\frac{\pi D}{\lambda} \right) + \log_{10} \eta \right) \\ = 20 \log_{10} \left(\frac{\pi D}{\lambda} \right) + 10 \log_{10} \eta$$

This derivation of an expression for gain of a non-uniformly illuminated circular aperture, with aperture efficiency η , demonstrates the significance of the terms in the expression for the gain of a conical aperture (Equation 2). The term $20 \log_{10} \frac{\pi D}{\lambda}$ is equivalent to that for the far field gain of a uniformly illuminated aperture of diameter D. The gain correction factor L (for a conical horn) may be assumed equivalent to $10 \log_{10} \frac{1}{\eta}$, the gain correction associated with the aperture efficiency η for the non-uniformly illuminated circular aperture. Therefore, using the diameter and flare length of the conical horn, the efficiency and effective area as well as gain of an equivalent circular aperture can be determined from the gain-correction factor vs. aperture phase deviation curve of Figure 1. Therefore, the aperture efficiency for the circular aperture equivalent of a conical horn can be expressed as

$$(11) \quad \eta = 10^{-L_{dB}/10}$$

It is of interest to apply the results of circular aperture theory, and the resulting model used for potential hazard evaluation of circular reflecting apertures [2,3] to the problem of determining the radiation characteristics of the conical horn antenna. An added advantage of being able to use such a model is that, in addition to being capable of determining far-field radiation characteristics for an aperture, the near field and transition region (transition between near and far field regions) characteristics can also be determined. The point source model is limited only to far field characteristics.

The near field on-axis power density is difficult to determine analytically for conical horn antennas. However, the non-uniform electric field distribution over the aperture, as evidenced by the distribution in Figure 3 [4], and the equivalence obtained from the expression for the gains of circular plane apertures and conical horns, allows a correspondence to be assumed between conical horn gain-correction factor and aperture efficiency for circular plane antennas. An approximation to near-field power density of a conical horn antenna can be obtained through the use of the expression (Equation 12) for the on-axis near field power density for a circular aperture with the same diameter modified by the equivalent aperture efficiency.

$$(12) \quad W_{nf} = \frac{16\eta P}{\pi D^2}$$

W_{nf} = on-axis near-field power density
P = power illuminating the reflector

The extent of the effective near field, R_1 , anticipated through the application of the circular aperture model is given by Equation 13.

$$(13) \quad R_1 = \frac{D^2}{4\lambda}$$

The associated anticipated radiation levels at near- and far-field locations for the traffic radar systems, using the expressions for W_{nf} and R_1 (Equations 12 and 13) and W_{ff} (Equation 14) associated with paraboloidal reflectors are presented in Table 4.

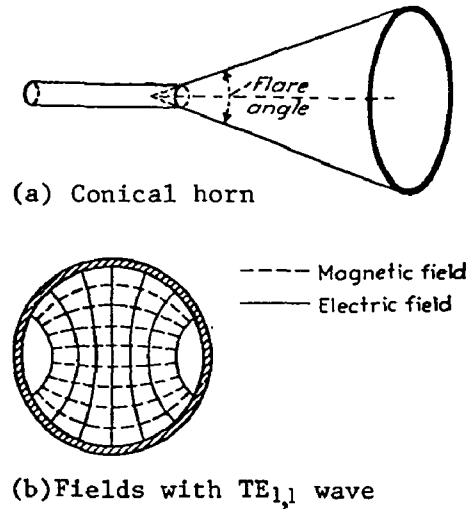


Fig. 3 Conical horn and field distribution within horn for $TE_{1,1}$ wave

$$(14) \quad W_{ff} = 2.47 W_{nf} \left(\frac{R_1}{R} \right)^2$$

The theoretical half-power beam width and relative intensity of the first side lobe below peak intensity are included for comparison with manufacturers specifications and values obtained using Figures 1 and 2.

Table 4. Anticipated Characteristics and Radiation Levels using Circular Aperture Theory

Anticipated Characteristics	TR6, MR7	MOVAR, Speedgun
Near-field extent (m)	.24	.091
Aperture efficiency	.67	.73
Near-field on-axis power density (W/m^2)	1.25×10^1	3.59×10^1
Beamwidth (degrees)	13.4	19.6
First sidelobe level (dB)	-24	-24
Power density (W/m^2) at various distances (m)		
.66	4.08	1.70
.91	2.15	8.92×10^{-1}
1.32	1.02	4.24×10^{-1}
2.67	2.49×10^{-1}	1.04×10^{-1}
28.3	2.22×10^{-3}	9.22×10^{-4}

The values for anticipated power density, using theoretically determined values for effective near field extent and power density, at any far field location agree within 3% with those calculated using the point source model (Equation 1) and the conical horn characteristics (Equation 2 and Figure 1) for a maximum source power of 0.1 W.

POWER DENSITY MEASUREMENTS

Values of power density in the near field and at several far field locations were measured for the radiation produced by the TR7 traffic radar system. The near field power density, as close to the horn axis as possible, was measured using the Narda Model 8321 broadband isotropic probe and the associated Model 8316 probe readout unit. The probe will measure power density to within ± 1.0 dB from energy incident in any direction (except from and through the handle) over a frequency range of 1 to 12 GHz. The near-field power density measured at a 9 cm separation between the aperture and probe center, was 0.4 mW/cm^2 . The same probe was used to measure the power density at 91 cm from the aperture and indicated a far-field power density of 0.025 mW/cm^2 .

On-axis far field power density was measured at distances (between aperture and detecting antenna) of 0.66, 1.32, 2.67, and 28.3 meters using as the detector a log periodic antenna, AEL Model APX 1293, connected to a Hewlett-Packard scanning spectrum analyzer, Model 141T, with Model 8555A RF plug-in and Model 8552B IF plug-in. The scan was approximately centered at 10.525 GHz and scanned over the frequency range 10.5225 to 10.5275 GHz with a scan width of 0.5 MHz/division over a 10 division CRT display. The power density was determined from the maximum (as a function of frequency) detected power, the antenna gain at 10.525 GHz, and the connecting cable attenuation at that frequency.

Antenna gain information was obtained from the manufacturers specifications. Cable attenuation was determined by laboratory measurement using the spectrum analyzer and a frequency source which generated 10 dBm of RF power at 10.525 GHz. The attenuation of the signal from the detecting antenna, due to the cable, varied between -14 and -22 dB and depended on the cable geometry and position. An attenuation factor of -18 dB appeared to be the most likely for the system used.

The measurement of far-field power density, using the spectrum analyzer, was performed in the field. The attempt was made to align the transmitting conical horn antenna axis and the detecting antenna axis so as to be co-linear. At small distances between source and detector, misalignment is probable simply because transmitted beam widths are roughly equivalent to the dimensions of the detector, making alignment difficult. It is likely that the detected field, while being part of the main beam, is not the on-axis field resulting in the measured power being significantly less than the maximum in the main beam. This effect is minimized at great distances where the main beam spread is large compared to detector cross section.

The horizontal component of the circularly polarized electric field was measured by the antenna at several distances from the traffic radar source. The final spectrum analyzer display of the detected signal in the horizontal plane is given in terms of dB above $1 \text{ } \mu\text{V}$. The power relative to 0 dBm (in units of mW) is obtained by subtracting 107 dB from this value. This is the factor equivalent to 1 mW in terms of dB above $1 \text{ } \mu\text{V}$ into a $50 \text{ } \Omega$ system. Power density is obtained by correcting for the signal attenuation in the cable connecting the antenna and spectrum analyzer ($\sim 18 \text{ dB}$ at 10.5 GHz) to obtain the total power detected, multiplying by a factor of two to obtain the total power due to the circularly polarized field, and dividing total power measured by the effective cross-sectional area of the antenna.

The effective area of the detecting antenna is determined from the specified gain at 10.525 GHz by the expression for gain (Equation 8), $A_{\text{eff}} = \frac{\lambda^2 G}{4\pi}$, where G is the absolute gain of the antenna. The detecting antenna has an effective area of 2.89 cm^2 for the specified gain of 6.5 dB at 10.525 GHz ($\lambda = 2.85 \text{ cm}$).

Table 5 presents the measured data, applied correction factors, resulting measured power, and resulting power density at the specified distances from the antenna. It also includes the measurements made using the Narda probe in the near field (at 3.5 inch; i.e., .089 m) of the conical horn antenna and at 0.91 m from the horn.

There are two apparent factors which can introduce the most error into the measurement of power density using the spectrum analyzer. One is the possible misalignment of the antenna axes for separation distances where the beam diameter at the detector is roughly

Table 5. Measurement Results

Distance (m)	.089*	.66	.91*	1.32	2.67	28.3
Power displayed (dBμV)	-	84	-	79	76	55
Corrected Power (dBμV) (+18 dB for cable atten.)	-	102	-	97	94	73
Power in horizontal plane (dBm) (-107 dB)	-	-5	-	-10	-13	-34
Power density (W/m ²) (horizontal plane power x2 and divided by antenna area)	4	2.19	2.5x10 ⁻¹	6.92x10 ⁻¹	3.47x10 ⁻¹	2.76x10 ⁻³

*Measured with isotropic probe.

an order of magnitude of greater than the actual diameter of the detector; i.e., for the separation distances up to 1.32 meters. The other is the uncertainty in the attenuation factor associated with the connecting cable; i.e., ± 4 dB.

COMPARISON OF RESULTS - ANALYTICAL AND MEASURED

The predicted values of power density at various distances from the source, based upon either the far field point source model using empirically determined gain correction factors for conical horns, or the potential hazard evaluation model for circular apertures are compared with the measured power densities at those distances in Table 6.

Table 6. Predicted and Measured MR7 Power Densities

	Power Density (W/m ²) at distances of:					
	.089 m	.66 m	.91 m	1.32 m	2.67 m	28.3 m
Point source model	-	4	2.1	1	2.44x10 ⁻¹	2.17x10 ⁻³
Hazard evaluation model - circular aperture	1.25x10	4.08	2.15	1.02	2.49x10 ⁻¹	2.22x10 ⁻³
Measurement	4	2.19	2.5x10 ⁻¹	6.92x10 ⁻¹	3.47x10 ⁻¹	2.76x10 ⁻³

It is expected that the effect of source and detection antenna misalignment should be least at the separation distance of 28.3 m, where in fact the difference between the measured and theoretically determined values of power density is ~21%, the least which occurs in all of the measurements using the spectrum analyzer. This leads to confidence in the use of the cable attenuation factor chosen, -18 dB, the most predominant value observed during the calibration measurement. The much greater differences observed at closer distances are most likely due to the not surprising misalignment factor.

The good agreement between: (1) measured power density and the predicted values obtained through the use of both the point source and equivalent circular aperture model at 28.3 m, and (2) the predicted far field characteristics at all distances for both models used, provides confidence in the near field characteristics predicted by the equivalent circular aperture model.

Comparison of the beamwidth and first sidelobe reduction factor for all systems considered in Table 1 indicates that the circular aperture model used is at least as good as the empirical data available for conical horns (Figure 2). Table 7 includes the beamwidth and sidelobe reduction factors provided by the manufacturers as well as those obtained from the empirical data and the circular aperture model.

Table 7. Beamwidth and Sidelobe Characteristics

	TR6, MR7		MOVAR, Speedgun	
	B.W. (deg)	Sidelobe Reduction (dB)	B.W. (deg)	Sidelobe Reduction (dB)
Manufacturer's data	12	-25	14 to 16	-24
Empirical characteristics	8.9	-14	14	-14
Circular aperture model	14	-24	20	-24

The comparisons made above lead to a lack of confidence in the measurements made with the Narda probe for this particular measurement. It is conceivable that the discrepancies in both near field (at .089 m) and far-field power density measurements are due to a lateral displacement of the probe elements relative to the antenna axis, resulting in reduced power densities (relative to on-axis values) being indicated.

EVALUATION AND CONCLUSIONS

Traffic radars, typified by the systems studied, are low power devices, incapable of producing environmental levels of microwave radiation greater than 10^{-2} W/m² (1 μ W/cm²) at distances where persons would normally be exposed during use of such systems. The maximum power density produced, determined through calculation, is 36 W/m² (3.6 mW/cm²) and occurs at distances 9 cm (3.6 inches) or less from the antenna. Exposure levels decrease rapidly at distances greater than 2 feet from the antenna where the maximum power density is less than 4 W/m² (.4 mW/cm²). At a distance of 14 feet, the maximum exposure level is less than 0.1 W/m² (10 μ W/cm²) and decreases to less than 0.01 W/m² (1 μ W/cm²) at 44 feet. The occupants of a moving vehicle being irradiated by a traffic radar are unlikely to be exposed to a power density as great as 0.01 W/m². In addition, the mitigating effect of vehicular shielding would further reduce the microwave radiation level inside the vehicle below the level which would exist outside of the vehicle at any distance from the antenna.

Police personnel whose job related responsibilities involve the use of the radar units could be exposed to power densities up to 36 W/m² (3.6 mW/cm²) in the main beam of the horn antenna at distances very close to the antenna if the system had been previously activated, a situation which could occur during system set-up and antenna adjustment. For comparison purposes, the threshold for exposure allowed by the OSHA occupational exposure standard [5] is 100 W/m² (10 mW/cm²) for exposure durations of 6 minutes or more. Greater occupational exposure levels are permissible under this standard for shorter time durations if the exposure level averaged over any possible 0.1 hour period does not exceed 100 W/m². Thus the highest exposure possible due to traffic radar system operation is well within current standards for occupational exposure.

Although the maximum power densities produced by typical traffic radars do not exceed or even equal the OSHA occupational exposure threshold, unnecessary microwave radiation exposure to operating personnel or others can be eliminated. This can be accomplished by making the traffic radar system inactive (no radiation being emitted) during set-up and adjustment, and at times when the system is not being used for its intended purpose, a practice consistent with the use of traffic radars.

In general, the environmental levels of microwave radiation (produced by traffic radars) to which most persons may be exposed are too low to be a health or environmental concern.

REFERENCES

1. Antenna Engineering Handbook, Henry Jasik, Ed., McGraw-Hill Book Company, New York, 1961.
2. Microwave Antenna Theory and Design, Samuel Silver, Ed., Dover Publications, Inc., New York, 1965.
3. Hankin, Norbert N., An Evaluation of Selected Satellite Communication Systems as Sources of Environmental Microwave Radiation, EPA-520/2-74-008, U.S. Environmental Protection Agency, Washington, DC, December 1974.
4. Radio Engineers' Handbook, Frederick E. Terman, McGraw-Hill Book Company, New York, 1943.
5. Department of Labor, Occupational Safety and Health Administration, Code of Federal Regulations, Title 29-Labor Part 1910.97, Nonionizing Radiation, Revised as of July 1, 1974.